

© 2021 IEEE. Personal use of this material is permitted. Permission from IEEE must be obtained for all other uses, in any current or future media, including reprinting/republishing this material for advertising or promotional purposes, creating new collective works, for resale or redistribution to servers or lists, or reuse of any copyrighted component of this work in other works.

Decentralized and Model-Free Federated Learning: Consensus-Based Distillation in Function Space

Akihito Taya, *Member, IEEE*, Takayuki Nishio, *Senior Member, IEEE*, Masahiro Morikura, *Member, IEEE*, and Koji Yamamoto, *Senior Member, IEEE*

Abstract—This paper proposes a decentralized federated learning (FL) scheme for Internet of everything (IoE) devices connected via multi-hop networks. FL has gained attention as an enabler of privacy-preserving algorithms, but it is not guaranteed that FL algorithms converge to the optimal point because of non-convexity when using decentralized parameter averaging schemes. Therefore, a distributed algorithm that converges to the optimal solution should be developed. The key idea of the proposed algorithm is to aggregate the local prediction functions, not in a parameter space but in a function space. Since machine learning tasks can be regarded as convex functional optimization problems, a consensus-based optimization algorithm achieves the global optimum if it is tailored to work in a function space. This paper at first analyzes the convergence of the proposed algorithm in a function space, which is referred to as a meta-algorithm. It is shown that spectral graph theory can be applied to the function space in a similar manner as that of numerical vectors. Then, a consensus-based multi-hop federated distillation (CMFD) is developed for neural network (NN) as an implementation of the meta-algorithm. CMFD leverages knowledge distillation to realize function aggregation among adjacent devices without parameter averaging. One of the advantages of CMFD is that it works even when NN models are different among the distributed learners. This paper shows that CMFD achieves higher accuracy than parameter aggregation under weakly-connected networks. The stability of CMFD is also higher than that of parameter aggregation methods.

Index Terms—machine learning, federated learning, knowledge distillation, consensus-based distributed optimization, multi-hop network, distributed learning, IoE

I. INTRODUCTION

THE Internet of everything (IoE) is a paradigm where all devices in our lives (e.g., machines, smartphones, cars, houses, and also humans) are connected and interact with each other. These devices have many various sensors to recognize the real-world and share their information. These data accelerate data-driven analysis and machine learning (ML). ML and particularly deep learning (DL) have succeeded in improving image processing dramatically, and they can be key technologies of semantic analysis, prediction, and many other tasks. IoE devices are able to provide ML agents

Akihito Taya is with the College of Science and Engineering, Department of Integrated Information Technology, Aoyama Gakuin University, Sagamihara 252-5258, Japan (e-mail: taya@it.aoyama.ac.jp)

Takayuki Nishio is with the Department of Information and Communications Engineering, School of Engineering, Tokyo Tech., Japan (e-mail: nishio@ict.e.titech.ac.jp)

Masahiro Morikura and Koji Yamamoto are with the Graduate School of Informatics, Kyoto University, Kyoto 606-8501, Japan (e-mail: kyamamot@i.kyoto-u.ac.jp)

Manuscript received April 19, 2005; revised August 26, 2015.

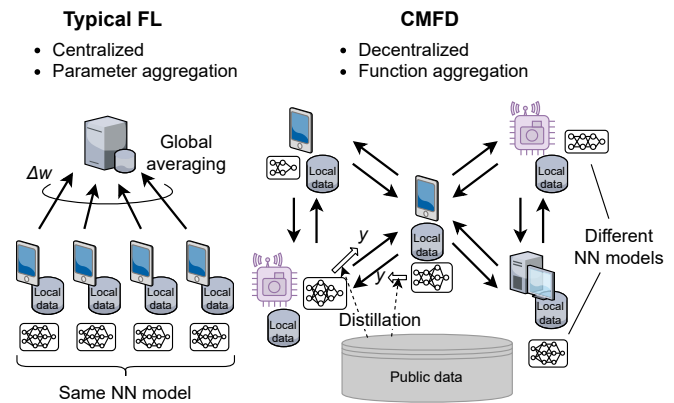


Fig. 1. Concept of CMFD. In typical FLs [1], devices send parameters to the server, and then the server aggregates them by averaging methods. In CMFD, the devices share output values with the adjacent devices via multi-hop networks and update their local models by a distillation method. CMFD realizes scalable and model-free FL systems.

with images, sound, physiological signals, and various data to train ML models. However, there are some challenges to utilize sensor data for ML. Protecting privacy is one of the most important problems. Users' photos, conversations, and behavior data stored in IoE devices, for example, are not preferable to be uploaded to data centers.

Federated learning (FL) has been proposed in order to avoid data uploading for preserving user privacy [1], [2]. Instead of collecting data to a server, FL updates neural network (NN) models at local devices (e.g., smartphones) using their private data and uploads the updated NN-parameters (i.e., weights and biases of each layer) to the server. Then, the server gathers and aggregates the uploaded parameters and broadcasts the up-to-date parameters to the local devices. This algorithm realizes distributed learning without exposing user data to the central learner. After the term FL is first introduced in [1], many kinds of FL have been developed to solve problems that appear in practical situations [2].

Typical FL schemes require a server to manage client devices and aggregate parameters, whereas IoE devices are expected to work without a server because they are sometimes connected via multi-hop networks. In multi-hop networks, the devices can directly communicate only with adjacent ones, and this constraint makes it difficult to adopt FL, which requires a central server [3]. Therefore, multi-hop FL algorithms, with which devices share information with only their adjacent devices, have been developed [3]–[6]. Multi-hop FLs can solve

TABLE I
ALGORITHM COMPARISON

	Network topology	Algorithm	Aggregation method	Model-free	IIDness	Convergence analysis
[1]	Star topology	Centralized	Parameter averaging	No	non-IID	N/A
[3]	Multi-hop	Decentralized	Parameter averaging	No	non-IID	N/A
[4], [5]	Multi-hop	Decentralized	Parameter averaging	No	non-IID	parameter convergence
[6]	Multi-hop	Decentralized	Parameter averaging	No	IID	N/A
[7]	Star topology	Centralized	Distillation	No	non-IID	N/A
[8]–[10]	Star topology	Centralized	Distillation	No ^a	non-IID	N/A
[11]	Star topology	Centralized	Distillation	Yes	non-IID	N/A
[12]	Multi-hop	Centralized	Distillation	No	non-IID	N/A
[13], [14]	Complete graph	Decentralized	Distillation	No ^a	IID	N/A
CMFD	Multi-hop	Decentralized	Distillation	Yes	non-IID	function convergence

^a It may be possible to implement, but not evaluated.

some problems of centralized FLs. Firstly, multi-hop FLs are not suffered from a communication bottleneck of the server. Therefore, it is easy to increase the number of FL-participating devices, and a large amount of training data can be utilized for learning. Secondly, considering that some information is sent to other devices even if it does not include private data, some users feel anxiety when sending information to other devices than acquaintances. For these reasons, the study of multi-hop FLs should be motivated to realize higher scalability and security than a centralized one.

Although multi-hop FL algorithms have been studied in [3]–[6], there remain the following challenges.

Model constraint: Existing works assume that all the devices have the same NN model architecture (e.g., the number of layers, hidden nodes, and how they are connected). However, considering that IoE devices have different computational resources, it is better to use different NN models depending on their computational capacities. Besides, if some IoE device vendors are collaborating in a single FL system, they might prefer to keep their NN models secret. Therefore, it is preferable to ease the constraint and make devices decide their NN models by themselves depending on their own conditions.

Convergence analysis under non-IID situation: The convergence of multi-hop FL is not guaranteed because multi-hop FL tasks are formulated as decentralized non-convex optimization problems. If centralized FL algorithms are adopted, all devices can synchronize their parameters at the end of each iteration because there is a parameter server, which manages and broadcasts a global model. In contrast, it is not generally guaranteed when using decentralized algorithms that all devices obtain the same model because there is no chance to synchronize all models. Besides, multi-hop FL is suffered from non-independent and identically distributed (IID) problems more severely than centralized FL. It is usual in FL that data distributions vary across devices because of users' interests and conditions [2]. Such a situation, called non-IIDness, deteriorates FL performance drastically, which has been widely studied [15]–[17]. In contrast to centralized FLs, FLs in multi-hop networks are further affected by non-IIDness, because NN models are shared only among adjacent devices.

We focus on these problems and propose a decentralized FL algorithm, which optimizes prediction functions in a *function space*. The proposed algorithm is referred to as a

meta-algorithm in this paper because it can be applied not only to NNs but also to other gradient-descent-based ML algorithms, such as gradient boosting decision tree (GBDT). The meta-algorithm aggregates the local prediction functions based on consensus-based distributed optimization (CDO) to guarantee convergence even under multi-hop networks. We mathematically analyze the convergence of the meta-algorithm in a function space because the convergence in a function space is practically sufficient, whereas the convergence in a parameter space is difficult to achieve.

We also develop consensus-based multi-hop federated distillation (CMFD) as an implementation of the meta-algorithm that can be applied to NN. Fig. 1 shows the overview of our CMFD, and the characteristics of CMFD are compared with other FL algorithms in Table I. CMFD leverages a distillation method to aggregate prediction functions. A distillation, or knowledge distillation, is a method that transfers knowledge acquired in a well-learned model to another model [18]. We adopt distillation to our algorithm because it can aggregate NN models even if their architectures are not the same. Distillation methods are applied in centralized FLs [7]–[11], [19], [20] because of its communication efficiency. However, a distillation-based FL under multi-hop networks has not been studied to the best of our knowledge.

A. Related works

Decentralized learning algorithms in multi-hop networks: Multi-hop FL is introduced in [3]–[6] for IoE devices. Savazzi *et al.* [3] developed a multi-hop FL algorithm that shares both model updates and gradients to improve convergence. Lalitha *et al.* [4] proposed a Bayesian approach to estimate the global model and tackle non-IID problems by updating and aggregating beliefs with neighbors. However, the evaluations were limited to a few nodes, and it is still uncertain whether the algorithm converges when there are many devices. Lian *et al.* [5] proposed parallel stochastic gradient descent (SGD) in multi-hop topologies and showed that decentralized parallel SGD (D-PSGD) speeded up learning when the channel capacity of the centralized server is a bottleneck because of narrow bandwidths. Sato *et al.* [6] extended D-PSGD to apply it to wireless networks by considering the channel capacity of each link. These algorithms are operated and analyzed in a parameter space, and thus they fundamentally require NN

model architectures to be the same among all devices, which decreases the flexibility of FL systems. In contrast to these algorithms, we utilize distillation to aggregate NN models in order to realize model-free FL.

Distillation: Distillation is originally utilized to make a copy of a prediction function, but it is also adopted to FL because of its communication efficiency. While typical FL needs to send all parameters of NN, distillation-based FL sends just the output of the prediction function, which usually has smaller dimensions than NN parameters. Therefore, federated distillation (FD) is proposed to realize communication efficient algorithms [7]–[11]. In order to address uplink-downlink capacity asymmetry, Mix2FLD proposed in [7] uses FL for downlink and FD for uplink. [8] proposes hybrid FD to compensate the performance gap between FL and FD by using the covariate information among the devices. [9] leverages unlabeled open data to realize semi-supervised FD. Cronus proposed in [11] leverages distillation in order to realize heterogeneous federated learning where different NN architectures are used. [10] proposes federated augmentation (FAug) by extending FD. FAug leverages generative adversarial network (GAN) to generate IID datasets while preserving privacy. FAug is extended to MultFAug in [12] to be used in multi-hop networks. MultFAug sends NN model information via multi-hop networks, but model aggregation is operated in a centralized manner. Such a centralized algorithm is not scalable to the number of devices because they are exposed to bottleneck problems when aggregating NN models.

In contrast to the above-mentioned works, which apply distillation to FL with star topologies, [13], [14] apply distillation to decentralized learning. These works show some advantages of distillation-based decentralized learning: speedup and cost-efficiency. However, the evaluations in [13], [14] assume fully-connected topologies and IID training data, which are not satisfied in IoE systems. Besides, if each device needs to share data with all the other devices, the amount of transferred data increases with the number of devices, and thus, the fully-connected algorithm cannot be applied to systems with a large number of devices. Our algorithm can be applied to devices connected via multi-hop networks, which is useful for IoE systems. We also show that CMFD can be regarded as a distributed optimization problem in a function space and provide a mathematical analysis of the convergence in a function space.

Distributed optimization: Distributed optimization problems have been discussed for wireless sensor networks (WSN), and many algorithms have been developed. One of these algorithms is called CDO, or gossip algorithms, which can solve convex optimization problems typically designed as follows:

$$\underset{\theta \in \mathbb{R}^n}{\text{minimize}} \sum_i F_i(\theta), \quad (1)$$

where the function F_i is only known to agent i , and each agent exchanges information with only one-hop neighbors [21]–[23]. With CDO, agents individually update parameters θ by gradient descent and then share the parameters with neighbors. These steps are iterated until the parameters converge to the

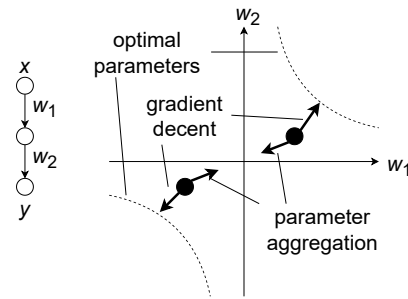


Fig. 2. A toy model of when parameter aggregation does not work well. Because there are two separated regions of optimal parameter pairs, the directions calculated by aggregation and gradient descent may differ.

optimal solution. Elgabli *et al.* proposed group alternating direction method of multipliers (GADMM), which used CDO to solve convex machine learning problems in [24]. CDO is also applied to multi-hop FLs by regarding F_i in (1) as a loss function with local private data and θ as the NN parameters [3], [4], [6].

However, training NN tasks become non-convex optimizations with such definition, and therefore, convergence is not guaranteed. Fig. 2 shows a simple example explaining why parameter aggregation in multi-hop networks does not work well. Consider a situation where the ground truth is $f(x) = x$, and prediction functions are represented as $f(x; w) = w_2 w_1 x$, where w_1 and w_2 are the parameters to be optimized. In this case, there are separated regions of optimal parameter pairs. When two devices are going to different optimal parameter pairs by gradient descent, the direction calculated by parameter aggregation can differ from that of the gradient descent updates and degrade performance.

B. Concept and contributions

A key idea of our proposal is *CDO in a function space* that optimizes not parameters but prediction functions themselves by regarding a supervised ML task as a functional optimization; that is, θ and F_i in (1) become prediction function f and loss functional L_i depending on local data, respectively as follows:

$$\underset{f \in \mathcal{F}}{\text{minimize}} \sum_i L_i(f), \quad (2)$$

where \mathcal{F} denotes a function space. Since commonly used ML criteria are convex functionals regarding a prediction function as an argument, it is expected that CDO in a function space can solve multi-hop FL in a decentralized manner. Our algorithm can learn with non-IID data because CDO is designed to work even when L_i are different among devices. Although there are some types of non-IIDness in FL context [2], feature and label distribution skew is considered in this paper; i.e., the distributions of features and labels vary across FL participants, whereas the conditional distribution of labels given feature values is the same among the participants. Image classifying is a typical task that this assumption holds. A label that the input image infer does not depend on devices, whereas image distributions are different among devices.

We first propose an algorithm that performs CDO in a function space, which is referred to as a meta-algorithm because it can be applied to not only NNs but other ML algorithms. Since typical ML tasks are convex functional optimization problems, the meta-algorithm, which works in a function space, can solve them, and the convergence is guaranteed. We mathematically prove the meta-algorithm convergence in a function space when devices have non-IID data. In order to analyze how local prediction functions get close in a function space by the meta-algorithm, we utilize spectral graph theory in the proof of Theorem 1. It is also notable that the meta-algorithm works in a decentralized manner and is scalable to the number of devices thanks to the CDO scheme.

Then, we develop a CMFD as a NN version of the meta-algorithm, because the meta-algorithm aggregate prediction functions directly in a function space, which cannot be realized when using NN. Distillation realizes function aggregation by adding outputs of prediction functions shared by the devices. Although distillation needs the same inputs to be shared, public open data can be utilized in order to avoid share private data [9]. Distillation also allows the devices to adopt different NN models because the devices do not directly share their parameters. Thus, each device can update the parameters of their NN models independently without caring parameters of other devices. This scheme relaxes the constraints of FL and is suitable for IoE systems where the devices have different computational resources.

The contributions of this paper are summarized as follows:

- In order to train ML models in a decentralized manner for IoE systems, we propose an algorithm that optimizes ML models in a *function space*, which we refer to as a meta-algorithm. The meta-algorithm adopts a CDO scheme to solve convex functional optimization problems under the condition where IoE devices communicate with their adjacent devices and update prediction functions without a coordinator.
- We analyze the convergence of the proposed meta-algorithm in a function space. The analysis is divided into two parts: the convergence among devices provided in Theorem 1 and the convergence to the global optimum provided in Theorem 2. By focusing on the behavior of gradient descent in a function space, we successfully prove the convergence of the meta-algorithm and provide an upper bound under non-IID situations. We utilize spectral graph theory to prove the convergence by defining a Cartesian product of the function spaces, which represents all prediction functions jointly. We show that the spectral of the defined space can be analyzed in a similar manner as numerical vectors.
- As an implementation of the meta-algorithm, we develop a CMFD for NNs, which leverages distillation to train NNs. Thanks to distillation, CMFD can be adopted even when the NN architectures are different among the devices. Therefore, CMFD suits IoE systems where devices with various computational resources are connected. We evaluate with ring lattice and scale-free networks, and it is confirmed that CMFD can learn with non-IID data even with heterogeneous NN models. The evaluations

show that CMFD archives high stability than parameter-aggregation-based multi-hop FL algorithms.

The rest of this paper is organized as follows: Problem definition is described in Section II. Then, the proposed algorithm is explained in Section III and evaluated in Section IV. Finally, the conclusions are drawn in Section V.

II. PROBLEM STATEMENT

We consider that IoE devices with sensors are connected via a multi-hop network, and each device i can communicate with only its adjacent devices \mathcal{N}_i in each step. Device i manages its prediction model f_i and updates f_i using its local data set \mathcal{D}_i by a ML scheme. The local data set should not be shared because it includes private information. Therefore, instead of sharing dataset \mathcal{D}_i , devices share some information representing f_i with their adjacent devices \mathcal{N}_i . By using the received information, the devices train their prediction model f_i to be optimal even if the local datasets are non-IID. The mathematical problem is formulated as the following.

Let $\mathcal{X} \subseteq \mathbb{R}^N$ and $\mathcal{Y} \subseteq \mathbb{R}^M$ be an input space (or a feature space) and an output space, respectively. We denote by $f : \mathcal{X} \rightarrow \mathcal{Y}$ a prediction function. Let $l(y, y') : \mathcal{Y} \times \mathcal{Y} \rightarrow \mathbb{R}$ be cost function of each element $y, y' \in \mathcal{Y}$. When the mean squared error (MSE) criterion is used, $l(y, y')$ is defined as $l(y, y') := \|y - y'\|^2$ and when the Kullback-Leibler (KL) divergence is used, defined as $l(y, y') := \sum_{m=1}^M y_m \log \frac{y_m}{y'_m}$, where y_m denotes the m th element of vector y . Here, a global loss functional $L_\mu(f)$ is defined as follows:

$$L_\mu(f) := \int_{\mathcal{X}} l(f(x), f^*(x)) d\mu, \quad (3)$$

where μ and f^* represent a global probability measure on \mathcal{X} and the ground truth function. Local loss functionals for each user $i \in \mathcal{U}$ are also defined as follows:

$$L_{\mu_i}(f) := \int_{\mathcal{X}} l(f(x), f^*(x)) d\mu_i, \quad (4)$$

where μ_i and \mathcal{U} represent a local probability measure of user i and a set of users, respectively. We denote by L_μ^2 the L^2 space with respect to μ and by $\langle \cdot, \cdot \rangle_{L_\mu^2}$ a inner product and norm are defined as $\langle f, g \rangle_{L_\mu^2} := \int_{\mathcal{X}} \langle f(x), g(x) \rangle_{\mathcal{Y}} d\mu$ and $\|f\|_{L_\mu^2} := \sqrt{\langle f, f \rangle_{L_\mu^2}}$, respectively where $\langle \cdot, \cdot \rangle_{\mathcal{Y}}$ represents the inner product in the vector space \mathcal{Y} .

This paper focuses on convex loss functionals in function space L_μ^2 because commonly used criteria (e.g., MSE and KL divergence [25]) are convex.

Assumption 1: $L_\mu(f)$ and $L_{\mu_i}(f)$ satisfy the following inequalities for all f_1, f_2 , and $t \in [0, 1]$:

$$L_\mu(tf_1 + (1-t)f_2) \leq tL_\mu(f_1) + (1-t)L_\mu(f_2), \quad (5)$$

$$L_{\mu_i}(tf_1 + (1-t)f_2) \leq tL_{\mu_i}(f_1) + (1-t)L_{\mu_i}(f_2). \quad (6)$$

We also assume that both of the global and local loss functionals are Lipschitz continuous in order to discuss the convergence of the gradient descent algorithm. In contrast to [5], which considers Lipschitz gradient continuity in a parameter space, we consider Lipschitz continuity in a function space.

Assumption 2: $L_{\mu_i}(f)$ satisfies the following Lipschitz condition for all f_1 and f_2 :

$$|L_{\mu_i}(f_1) - L_{\mu_i}(f_2)| \leq K_i \|f_1 - f_2\|_{L_{\mu_i}}, \quad (7)$$

where K_i denotes the Lipschitz constant of $L_{\mu_i}(f)$.

In the considered system, it is assumed that the ground truth function is common among users, but probability measures μ_i vary across users, i.e., users have non-IID data. This setting is referred to as ‘‘feature distribution skew’’ and ‘‘label distribution skew’’ in [2]. Considering the meaning of global probability measure, it is empirically represented as follows:

$$\mu = \frac{1}{n} \sum_{i \in \mathcal{U}} \mu_i, \quad (8)$$

where n represents a number of users. Using (8), global loss functional $L_{\mu}(f)$ can be written as $L_{\mu}(f) = \frac{1}{n} \sum_{i \in \mathcal{U}} L_{\mu_i}(f)$. It is also notable that μ_i is absolutely continuous with respect to μ ($\mu_i \ll \mu$) and there exists Radon-Nikodym derivative $\nu_i = \frac{d\mu_i}{d\mu}$ for all $i \in \mathcal{U}$. We denote by S_i the supremum of $\nu_i(x)$, i.e., $S_i := \sup_{x \in \mathcal{X}} \nu_i(x)$. This value is regarded as a metric of non-IIDness because it takes the minimum value 1 when μ_i and μ are the same.

In ML context, because true loss functional $L_{\mu}(f)$ cannot be obtained, the following approximation, called empirical risk, is used:

$$\begin{aligned} L_{\mu}(f) &\approx \frac{1}{|\mathcal{D}|} \sum_{(x,y) \in \mathcal{D}} l(f(x), y) \\ &= \frac{1}{n} \sum_{i \in \mathcal{U}} \frac{1}{|\mathcal{D}_i|} \sum_{(x,y) \in \mathcal{D}_i} l(f(x), y), \end{aligned} \quad (9)$$

where \mathcal{D}_i , \mathcal{D} , and $|\cdot|$ denote a labeled data set of each device, the union of all the data sets \mathcal{D}_i , and the cardinality of a set, respectively. Here, we assume $|\mathcal{D}_i| = \frac{1}{n}|\mathcal{D}|$ for all $i \in \mathcal{U}$ for simplicity, but it is easily extended to general cases. When f is represented by a NN model with parameter vector w , the optimization problem is defined in a parameter space instead of the function space as follows:

$$\underset{w \in \mathbb{R}^{n_w}}{\text{minimize}} \quad L_{\mu}(f(\cdot; w)), \quad (10)$$

where n_w denote the number of parameters. In order to realize FL under multi-hop networks, this optimization problem should be solved under constraints that each device i shares some kind of information only with its adjacent devices denoted by \mathcal{N}_i .

[3], [4] apply CDO to solve (10) in a distributed way. Such algorithms, however, do not efficiently work because objective functions are not convex in a parameter space, and CDO cannot be generally applied to non-convex optimization problems. Thus, CDO in a parameter space can achieve only low performance in ML context, especially when the local data is non-IID. In contrast to conventional works that optimize parameters w , we develop an algorithm that optimize f directly. Considering that CDO achieves an optimal solution when the objective function is convex, the following optimization problem is expected to be solved,

$$\underset{f \in L_{\mu}^2}{\text{minimize}} \quad L_{\mu}(f). \quad (11)$$

The following section explains how to solve this optimization problem, and prove convergence of the proposed algorithm.

III. CONSENSUS-BASED MULTI-HOP FEDERATED LEARNING

A. Meta-algorithm in a function space

At first, we explain a meta-algorithm in a function space L_{μ}^2 to solve (11) and prove that the prediction functions of all devices converge to the optimal solution. Then, distillation is introduced in Sec. III-C in order to apply the proposed meta-algorithm to NN models.

In order to solve (10), existing CDO-based FLs in a parameter space [3]–[6] basically update local models by following equations:

$$\hat{w}_i^{t+1} \leftarrow w_i^t - \eta_t \nabla_w \sum_{(x,y) \in \mathcal{D}_i} l(f(x; w_i^t), y), \quad (12)$$

$$w_i^{t+1} \leftarrow \hat{w}_i^{t+1} - \varepsilon \sum_{j \in \mathcal{N}_i} (\hat{w}_i^{t+1} - \hat{w}_j^{t+1}), \quad (13)$$

where w_i^t , \hat{w}_i^t , and η_t represent parameters of device i at epoch t , temporal parameters, and a learning rate, respectively. We assume η_t monotonically decreases, and therefore η_t satisfies $\eta_t \leq \eta_1$. Coefficient ε of the second term of (13) is referred to as sharing rate, which adjusts convergence among devices. In order to operate (12) and (13), \hat{w}_i^t should be shared among adjacent devices, and thus wide communication bandwidths is required when a NN model has many layers. Besides, CDO is not guaranteed to reach the optimal solution for non-convex optimizations.

To tackle these problems, we replace parameter optimization by function optimization as follows:

$$g_i^{t+1} \leftarrow f_i^t - \eta_t d_i^t \nu_i, \quad (14)$$

$$f_i^{t+1} = g_i^{t+1} - \varepsilon n_i \left(g_i^{t+1} - \frac{1}{n_i} \sum_{j \in \mathcal{N}_i} g_j^{t+1} \right), \quad (15)$$

where n_i represents the number of neighbors of user i defined by $n_i := |\mathcal{N}_i|$. Here, $d_i^t \in \partial L_{\mu_i}(f_i^t)$ represents a Fréchet subgradient of the local loss functional $L_{\mu_i}(f)$, which satisfies the following inequality [26]:

$$\forall h \in L_{\mu_i}^2, \langle d_i^t, h - f_i^t \rangle_{L_{\mu_i}^2} \leq L_{\mu_i}(h) - L_{\mu_i}(f_i^t). \quad (16)$$

In (14), $\nu_i = \frac{d\mu_i}{d\mu}$ converts a subgradient d_i^t in metric space $L_{\mu_i}^2$ to that in L_{μ}^2 . We assume ε in (15) satisfies $0 < \varepsilon \leq \frac{1}{2\Delta}$ where Δ denotes the maximum degree of the network graph. This condition is required to guarantee convergence, which is explained in Sec. III-B.

Algorithm 1 shows a pseudo code applying the above operation. In each epoch, devices update their local prediction functions f_i^t by (14) (step 3–4). After updating local prediction functions, the devices share their temporal functions g_i^{t+1} with adjacent devices \mathcal{N}_i (step 5). Then, the devices aggregate the received models, and calculate the weighted average of the prediction functions (step 8). After iterating these steps, all the local prediction functions converge to the optimal solution f^* of (11).

Algorithm 1 Meta-algorithm of consensus-based multi-hop FL in a function space

Require: Loss functional: $L_{\mu_i}(\cdot)$,
 Probability density function: μ_i, μ
 Learning and sharing rate: η_t, ε

- 1: **while** not converged **do**
- 2: **for all** device $i = 1, \dots, n$ **do**
- 3: $d_i^t \leftarrow \partial L_{\mu_i}(f_i^t)$
- 4: $g_i^{t+1} \leftarrow f_i^t - \eta_t d_i^t \nu_i$
- 5: Send g_i^t to neighbor devices
- 6: **end for**
- 7: **for all** device $i = 1, \dots, n$ **do**
- 8: $f_i^{t+1} \leftarrow g_i^{t+1} - \varepsilon n_i \left(g_i^{t+1} - \frac{1}{n_i} \sum_{j \in \mathcal{N}_i} g_j^{t+1} \right)$
- 9: **end for**
- 10: **end while**

B. Convergence analysis of the meta-algorithm

The analysis of the convergence is divided into two parts. First, we obtain an upper bound of the distance between the local prediction functions f_i^t and their average \bar{f}_t . Then, we discuss the limits of $L_\mu(\bar{f}_t)$ as $t \rightarrow \infty$.

In order to mathematically analyze the convergence of the meta-algorithm, we define a federated function \mathbf{f}_t as a tuple of prediction functions:

$$\mathbf{f}_t := (f_1^t, \dots, f_n^t)^T \in \Phi_n := (L_\mu^2)^n, \quad (17)$$

where $[\cdot]^T$ denotes the transpose of $[\cdot]$. Φ_n is the n -ary Cartesian power of L_μ^2 with inner product $\langle \mathbf{a}, \mathbf{b} \rangle_{\Phi_n} := \sum_{i=1}^n \langle a_i, b_i \rangle_{L_\mu^2}$ and norm $\|\mathbf{a}\|_{\Phi_n} := \sqrt{\langle \mathbf{a}, \mathbf{a} \rangle_{\Phi_n}}$ where a_i and b_i are the i th elements of federated functions \mathbf{a} and $\mathbf{b} \in \Phi_n$, respectively. Addition and scalar multiplication of federated functions are calculated in element-wise manners. Product of matrices and federated functions is defined in similar manner as that of matrices and numerical vectors, i.e., the i th element of $\mathbf{A}\mathbf{a} \in \Phi_n$ is defined as $\sum_{j=1}^n A_{ij}a_j$, where A_{ij} denotes the (i, j) element of the matrix A .

We have the following lemma about the relation between the induced norm of real matrices and federated functions.

Lemma 1: Let $\|A\|$ be the induced norm of matrix $A \in \mathbb{R}^{n \times n}$ corresponding to the 2-norm of real vectors, i.e.,

$$\|A\| := \max \left\{ \frac{\|A\mathbf{v}\|_{\mathbb{R}^n}}{\|\mathbf{v}\|_{\mathbb{R}^n}} \mid \mathbf{v} \in \mathbb{R}^n, \mathbf{v} \neq \mathbf{0} \right\}. \quad (18)$$

Then, $\|A\|$ is also the induced 2-norm of federated functions, i.e., $\|A\|$ satisfies

$$\|A\| = \max \left\{ \frac{\|A\mathbf{a}\|_{\Phi_n}}{\|\mathbf{a}\|_{\Phi_n}} \mid \mathbf{a} \in \Phi_n, \mathbf{a} \neq \mathbf{0} \right\}. \quad (19)$$

Proof: See Appendix A. ■

This lemma enables us to analyze the convergence of Algorithm 1 in Φ_n in a similar manner as in \mathbb{R}^n .

Using federated functions, (14) and (15) can be rewritten as follows:

$$\mathbf{g}_{t+1} \leftarrow \mathbf{f}_t - \eta_t \mathbf{d}_t, \quad (20)$$

$$\mathbf{f}_{t+1} \leftarrow \mathbf{g}_{t+1} - \varepsilon L \mathbf{g}_{t+1} = (I - \varepsilon L) \mathbf{g}_{t+1}, \quad (21)$$

where \mathbf{g}_t , \mathbf{d}_t , I , and L denote federated functions whose i th elements are g_i^t and $d_i^t \nu_i$, the identity matrix, and the Laplacian matrix of the network graph, respectively. The (i, j) th element of L is given by

$$L_{ij} := \begin{cases} |\mathcal{N}_i| & \text{if } i = j \\ -1 & \text{if } j \in \mathcal{N}_i \\ 0 & \text{otherwise.} \end{cases} \quad (22)$$

Let λ_2 denote the second minimum eigenvalue of L , which is also known as the algebraic connectivity [27]. Generally, consensus algorithms converge faster if this value becomes large.

We denote by $\bar{\mathbf{a}}$ a mean federated function whose elements are the mean of functions a_i , which is calculated as $\bar{\mathbf{a}} := \frac{1}{n} \mathbb{1}_{n \times n} \mathbf{a}$, where $\mathbb{1}_{n \times n}$ represent an $n \times n$ matrix of ones. Using federated functions, the root-mean square distance between the local prediction functions and the mean of them are expressed as follows:

$$D_t := \sqrt{\frac{1}{n} \sum_{i=1}^n \|f_i^t - \bar{f}_t\|_{L_\mu^2}^2} = \frac{1}{\sqrt{n}} \|\mathbf{f}_t - \bar{\mathbf{f}}_t\|_{\Phi_n}, \quad (23)$$

where \bar{f}_t denotes the mean of f_i^t . Thanks to Lemma 1, the upper bound of D_t can be obtained in a similar manner as if federated function \mathbf{f}_t were a numerical vector using spectral graph theory.

Theorem 1: If the network graph is connected, the sharing rate satisfies $0 < \varepsilon \leq \frac{1}{2\Delta}$, and Assumptions 1 and 2 hold, D_t is upper bounded as follows:

$$D_t \leq \frac{1}{\sqrt{n}} \|\mathbf{f}_1\|_{\Phi_n} \kappa_2^{t-1} + K_m \sum_{\tau=1}^{t-1} \eta_\tau \kappa_2^{t-\tau}, \quad (24)$$

where we define $\kappa_2 := 1 - \varepsilon \lambda_2$ and $K_m := \max_i \{S_i K_i\}$.

Proof: See Appendix B. ■

Because λ_2 does not exceed the double of the maximum degree Δ of the network graph, if the sharing rate ε is selected to satisfy $0 < \varepsilon \leq \frac{1}{2\Delta}$, we have $0 \leq \kappa_2 < 1$. Since we assume learning rate η_t monotonically decreases, the right hand side of (24) is bounded as follows:

$$\begin{aligned} \gamma_t &:= \frac{1}{\sqrt{n}} \|\mathbf{f}_1\|_{\Phi_n} \kappa_2^{t-1} + K_m \sum_{\tau=1}^{t-1} \eta_\tau \kappa_2^{t-\tau} \\ &\leq \frac{1}{\sqrt{n}} \|\mathbf{f}_1\|_{\Phi_n} \kappa_2^{t-1} + K_m \eta_1 \frac{\kappa_2(1 - \kappa_2^{t-1})}{1 - \kappa_2}. \end{aligned} \quad (25)$$

The limit of D_t is bounded by the constant value as follows:

$$\lim_{t \rightarrow \infty} D_t \leq \frac{\eta_1 \kappa_2 K_m}{1 - \kappa_2} = \frac{\eta_1 (1 - \varepsilon \lambda_2) K_m}{\varepsilon \lambda_2}. \quad (26)$$

Next, we discuss the optimality of \bar{f}_t . Since the sub-gradient method is not a descent method, we consider the best solution found so far in a similar manner as discussed

Algorithm 2 Pseudo code of CMFD

Require: Prediction function with NN parameters $w: f(\cdot; w)$,
 Cost function: $l(y, y')$
 Local and shared train data: $\mathcal{D}_i, \mathcal{D}_s$,
 Learning and sharing rate: η_t, ε

- 1: **while** not converged **do**
- 2: **for all** device $i = 1, \dots, n$ **do**
- 3: **for** minibatch $\hat{\mathcal{D}}$ in \mathcal{D}_i **do**
- 4: $\hat{w}_i^t \leftarrow w_i^t - \eta_t \nabla_w \sum_{(x,y) \in \hat{\mathcal{D}}} l(f(x; w_i^t), y)$
- 5: **end for**
- 6: **for all** $x \in \mathcal{D}_s$ **do**
- 7: $\hat{y}_{i,x}^t \leftarrow f(x; \hat{w}_i^t)$
- 8: **end for**
- 9: send $\hat{y}_{i,x}^t$ to neighbor devices
- 10: **end for**
- 11: **for all** device $i = 1, \dots, n$ **do**
- 12: receive $\hat{y}_{j,x}^t$ from neighbor devices
- 13: $c(\hat{w}_i) := \sum_{(x,y) \in \mathcal{D}_s} \left\| f(x; \hat{w}_i^t) - \frac{1}{n_i} \sum_{j \in \mathcal{N}_i} \hat{y}_{j,x}^t \right\|^2$
- 14: $w_i^{t+1} \leftarrow \hat{w}_i^t - \varepsilon n_i \nabla_w c(\hat{w}_i)$
- 15: **end for**
- 16: **end while**

in [28]. The best solution $f_{\text{best},t}$ is defined as $f_{\text{best},t} := \arg \min_{\tau=1, \dots, t} \{L_\mu(\bar{f}_\tau)\}$.

Theorem 2: The best solution $f_{\text{best},t}$ found in t -time iterations by Algorithm 1 satisfies the following inequality:

$$\begin{aligned} & L_\mu(f_{\text{best},t}) - L_\mu(f^*) \\ & \leq \frac{1}{2 \sum_{\tau=2}^t \eta_\tau} \left[C_1 + K_m \sum_{\tau=2}^t \eta_\tau^2 \right. \\ & \quad \left. + C_2 (1 - \kappa_2^{t-1}) \left(\eta_1 \|\mathbf{f}_1\|_{\Phi_n} + \sqrt{n} K_m \sum_{\tau=1}^{t-1} \eta_\tau^2 \right) \right], \end{aligned} \quad (27)$$

where C_1 and C_2 are defined as $C_1 := \|\bar{f}_2 - f^*\|_{L_\mu^2}^2$ and $C_2 := \frac{4K_m \kappa_2}{1 - \kappa_2}$, respectively.

Proof: See Appendix C. ■

When learning rate η_t satisfies $\sum_{t=1}^\infty \eta_t^2 < \infty$ and $\sum_{t=1}^\infty \eta_t = \infty$, the right-hand side of (27) converges to zero as $t \rightarrow \infty$. In contrast, when the constant learning rate is adopted, i.e., $\eta_t = \eta$ for all t ,

$$\begin{aligned} & \lim_{t \rightarrow \infty} L_\mu(f_{\text{best},t}) - L_\mu(f^*) \\ & \leq \frac{\eta K_m}{2} \left(1 + \frac{4\sqrt{n} K_m (1 - \varepsilon \lambda_2)}{\varepsilon \lambda_2} \right). \end{aligned} \quad (28)$$

Although it is not guaranteed that $L_\mu(\bar{f}_t)$ strictly decreases by the subgradient method, we can obtain decreasing series by tuning the learning rate.

C. CMFD as an implementation for neural networks

Since prediction functions are updated directly in Algorithm 1, an implementation scheme that updates the parameters

TABLE II
SIMULATION PARAMETERS

Parameters	Values
Num. devices	10
Network topology	Ring lattice, BA network
Num. public data $ \mathcal{D}_s $	1000
Num. local data $ \mathcal{D}_i $	1000
Num. labels of local data	2
Learning rate η	0.01, 0.1 (constant)
Sharing rate ε	0.001–6 (constant)
Optimizer	SGD
Minibatch size	100
Dropout rate	0.5 (CNN), 0.1 (FC)

of the NN models is required. We develop CMFD to realize aggregation of NN models by leveraging distillation. The pseudo code of the proposed algorithm is shown in Algorithm 2. First, we simply substitute the Fréchet subgradient by stochastic gradient in a parameter space (step 3–5). Device i updates its local prediction models $f(\cdot; w_i)$ using local dataset \mathcal{D}_i . In order to aggregate the prediction models, devices share input and output pairs of their prediction models instead of the parameters. Here, we utilize public dataset \mathcal{D}_s to aggregate prediction models by distillation. The devices calculate outputs $\hat{y}_{i,x}^t$ of public dataset \mathcal{D}_s , and send them to their neighbors \mathcal{N}_i (step 6–9). Using the received values, the devices update their models by distillation as follows:

$$c(\hat{w}_i) := \sum_{(x,y) \in \mathcal{D}_s} \left\| f(x; \hat{w}_i^t) - \frac{1}{n_i} \sum_{j \in \mathcal{N}_i} \hat{y}_{j,x}^t \right\|^2, \quad (29)$$

$$w_i^{t+1} \leftarrow \hat{w}_i^t - \varepsilon n_i \nabla_w c(\hat{w}_i), \quad (30)$$

where $c(\hat{w}_i)$ denotes a loss function of distillation. MSE is used as a loss function because it is an empirical representation of the L_μ^2 distance between two functions. Since the gradient of $c(\hat{w}_i)$ corresponds to the second term of (15), local models $f(\cdot; \hat{w}_i)$ is updated to get close in a function space by a gradient descent manner. In distillation process, public dataset \mathcal{D}_s is required to approximate distance in L_μ^2 by MSE, because if local dataset \mathcal{D}_i is used, MSE would be an approximation of $L_{\mu_i}^2$ rather than L_μ^2 . In addition, local datasets cannot be shared because they may include private information. Note that, labels are not required for public datasets, and thus, it is easy to collect. After sufficient iterations of the SGD with local dataset and distillation with public datasets, all the local models are expected to converge to the optimal solution of (11), even though parameters w_i do not converge to the same values by Algorithm 2.

IV. PERFORMANCE EVALUATION

We evaluated CMFD using public datasets MNIST [29] and fashion MNIST (F-MNIST) [30]. Simulation parameters are listed in Table II. We assumed ten devices were connected via multi-hop networks shown in Fig. 3. We evaluated ring lattice networks (R1, R2, and R3) and scale-free networks (BA1 and BA2), which are sometimes adopted to WSN for energy efficiency [31]. Evaluated scale-free networks were generate by Barabási–Albert (BA) algorithm [32]. In our simulations,

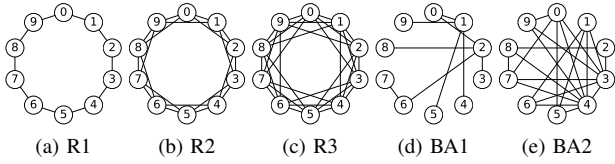


Fig. 3. Evaluated network topologies. R1, R2, and R3 are ring lattice networks, and BA1 and BA2 are scale-free networks generated by BA algorithm.

devices had two types of labels to evaluate non-IID situations. When evaluating ring networks, device $\#i$ ($\neq 9$) possessed training data labeled i and $i + 1$ and device $\#9$ used data labeled 9 and 0, assuming a situation where near devices had similar data distributions. On the other hand, when evaluating scale-free networks, two types of labels were chosen randomly. There were 1000 public data without ground truth labels that are used for distillation. The local datasets and the public dataset are allowed to duplicate. The NN layer architecture was CNN(32, 5)-CNN(64, 5)-FC(512)-FC(10)¹. ReLU was used as activation functions.

As a parameter-averaging algorithm in multi-hop networks, we evaluated performance of CDO in a parameter space, with which devices updated their parameterized by (12) and (13). When evaluating the parameter-averaging method, the initial parameters are set to be the same in order to avoid performance deterioration [1].

A. Convergence performance

Convergence performances of accuracy evaluated with MNIST and F-MNIST are shown in Fig. 4. As a baseline, the performances of the parameter-averaging method are shown in the right column. Each line in the figures indicates the accuracy of each device. We manually tuned sharing rate ϵ for learning rate $\eta = 0.01$ and 0.1. When comparing Figs. 4(a) and 4(c), accuracy increases faster when the network connectivity is large. The same behavior can be seen when learning F-MNIST. Not surprisingly, trained models of ten devices get close faster when the network becomes dense. Therefore, each device can increase the prediction accuracy of unknown labels that the device does not have. It is also shown that the fluctuation range of CMFD was smaller than that of the parameter-averaging algorithm.

Table III shows the average accuracy and other two metrics at the 1000 epoch with various parameters. ‘‘Max-min’’ is the difference of accuracies between the best and the worse devices, which is a metric of convergence among devices. ‘‘Deviation’’ is the averages of the last 100-epoch standard deviation of each device’s accuracy. From max-min values, it can be said that the accuracies of ten devices converged in smaller ranges with CMFD than the parameter averaging when the learning rate and the sharing rate were well-tuned. The fluctuation range of CMFD is about one-tenth of that of parameter-averaging by comparing deviations of two methods. The reason why the difference in stability occurs is that the

¹CNN(f, k) and FC(n) represent convolution layer with f -filters whose kernel size is $k \times k$ and fully connected layer with n -hidden nodes.

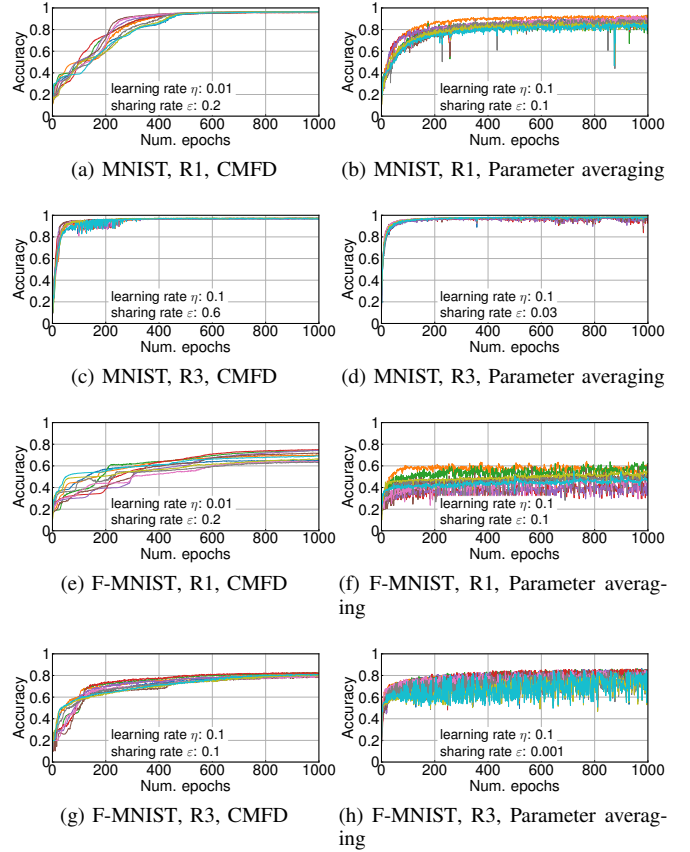


Fig. 4. Accuracies as functions of the number of epochs. Each line shows the accuracy of each device. Difference among devices with CMFD is smaller than that with the parameter averaging method. CMFD also achieves smaller fluctuation in time series. Comparing network topology R1 and R3, the strongly connected network R3 converges faster than R1.

parameter-averaging algorithm tries to solve a non-convex optimization problem, whereas CMFD is designed to solve a convex optimization problem in a function space. Since there are multiple local optima in a parameter space, when the parameters of devices tried to go to different optima, parameter-updating directions calculated by the parameter sharing and the gradient descent can be completely different. On the other hand, the local prediction functions of devices get close in a function space by CMFD, which allows different parameters as far as they are located in the same point in a function space.

B. Heterogeneous situation

Fig. 5 shows accuracies as the functions of sharing rate with different types of NN models. The layer architecture of model A was CNN(32, 5)-CNN(64, 5)-FC(512)-FC(10), which is the same as the previous evaluation. Model B was evaluated as a shallow NN, whose layer architecture was CNN(8, 5)-FC(32)-FC(10). The green and blue lines show the accuracies when all the devices adopt models A and B, respectively. The red line shows the accuracies when half of the ten devices adopt model A and the others adopt model B considering a situation where the devices have different computational resources. In the evaluation, the devices whose index were even number had rich resources and adopted model A, and the others had

TABLE III
ACCURACIES WITH VARIOUS PARAMETERS

		CMFD							Parameter averaging							
		Learning rate η		Sharing rate ε					0.01		0.1		Best acc.			
		0.01	0.1	0.01	0.1	0.01	0.1	1	0.001	0.01	0.1	0.001	0.01	0.1	Best acc.	
MNIST	R1	Accuracy (%)	38.3	91.2	83.1	21.5	87.4	95.0	96.3	61.3	63.6	64.1	83.6	85.0	86.7	86.7
		Max-min (pp)	28.8	8.7	15.6	17.8	18.9	3.6	1.0	11.6	11.8	19.3	13.9	13.4	7.5	7.5
		Deviation (pp)	0.8	0.2	1.1	0.0	0.3	0.2	0.1	1.2	1.3	1.1	4.0	2.3	1.6	1.6
	R3	Accuracy (%)	92.1	95.7	81.0	85.4	96.8	78.7	96.9	90.4	89.1	83.3	97.7	97.7	97.8	97.9
		Max-min (pp)	6.6	1.0	8.6	16.3	0.8	9.9	0.7	4.6	6.6	17.5	2.5	3.2	0.7	1.3
		Deviation (pp)	0.7	0.1	0.7	0.9	0.1	0.5	0.1	1.5	1.5	1.6	1.2	0.4	0.3	1.0
F-MNIST	R1	Accuracy (%)	30.9	60.6	64.1	20.8	39.7	62.4	69.2	44.1	44.4	45.4	51.4	50.3	51.9	51.9
		Max-min (pp)	21.3	15.7	26.0	10.8	36.7	26.4	12.2	13.9	12.4	13.0	18.9	15.8	15.7	15.7
		Deviation (pp)	0.2	0.3	0.4	0.0	0.2	0.8	0.2	0.9	0.8	0.7	3.2	3.1	2.8	2.8
	R3	Accuracy (%)	60.6	77.2	62.8	38.9	80.6	62.8	80.6	67.3	65.7	65.9	82.1	80.9	74.6	82.1
		Max-min (pp)	13.7	5.1	9.3	37.7	3.8	11.3	3.8	12.6	18.4	12.5	9.5	6.9	18.5	9.5
		Deviation (pp)	0.3	0.3	0.7	0.3	0.3	0.5	0.3	2.0	1.7	1.3	5.8	5.6	6.9	5.8

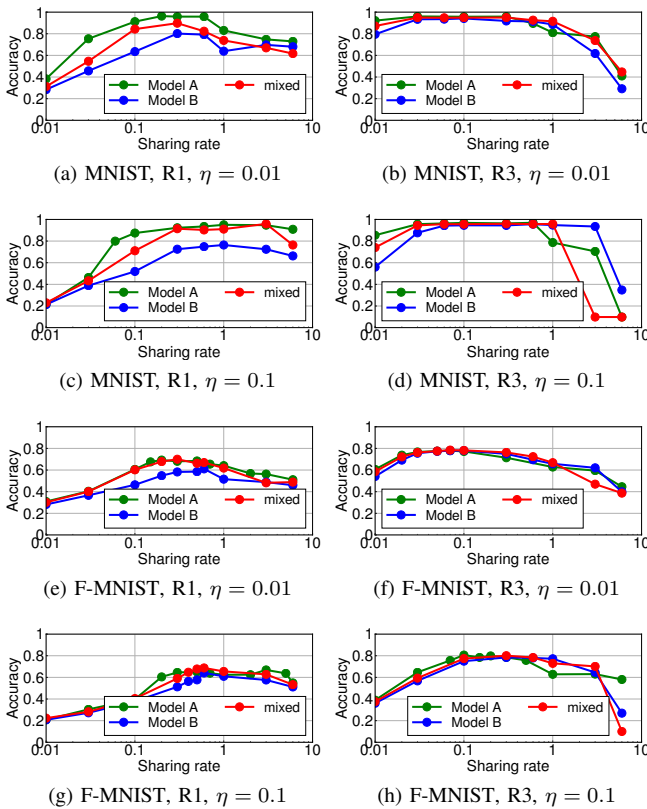


Fig. 5. Accuracies when different models are adopted. Because Model A is complex than Model B, Model A tends to achieve higher performance than Model B, especially when the devices are weakly connected. Under the heterogeneous situation, devices using Model B also achieve similar accuracy with those using Model A.

poor resources and adopted shallow NN model B. CMFD works even when devices adopt different NN models, whereas FL algorithms using parameter-averaging require the devices to adopt the same NN model. Since model B is shallow, the accuracies are lower than those with model A when the network topology is R1. In contrast, the connectivity becomes large, the accuracies of model B increased to the same level

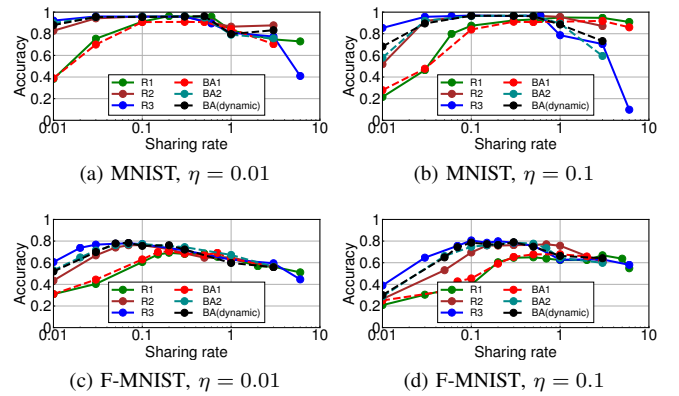


Fig. 6. Accuracies as functions of sharing rate with various topologies. When the network is strongly connected, the accuracy increases. It also can be said that there is no difference between stable and unstable networks.

TABLE IV
CONNECTIVITY OF TOPOLOGIES

Topology	R1	R2	R3	BA1	BA2
Algebraic connectivity	0.38	1.76	4.38	0.18	1.42
Average of degrees	2	4	6	1.8	4.2

as model A. This infers that the restrictions of local training disturbed learning, and the shallow model could not bring out its potential. When the two types of models are adopted by the different devices, the performances which adopted model B also achieved nearly the same performance as those with model A. Such characteristics are convenient where IoE devices with different computational resources cooperatively learn the same task.

C. Comparison with various sharing rate

Various topologies are compared in Fig. 6, which shows average accuracies as functions of sharing rate. The accuracies indicated by label “BA (dynamic)” show the performance when network topology dynamically changed at each epoch to evaluate situations where the mobile devices were moving

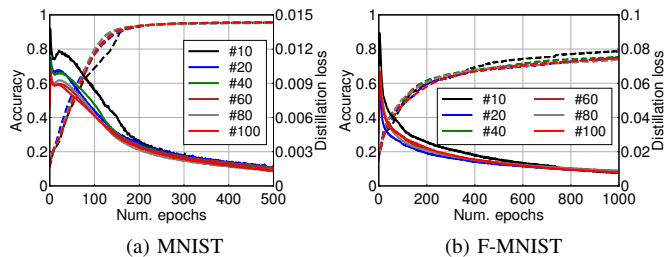


Fig. 7. Accuracies with various number of devices. The dotted lines show the average accuracies among all devices, and the solid lines show the average distillation losses. Both accuracies and distillation losses show similar values even when the number of devices increased because the networks had similar algebraic connectivity regardless of the number of devices. This means that the learning performance is scalable to FL participants.

TABLE V
CONNECTIVITY WITH THE VARIOUS NUMBER OF DEVICES.

Num. devices	10	20	40	60	80	100
Algebraic connectivity	1.41	1.44	1.40	1.37	1.35	1.32
Average of degrees	4.2	5.1	5.55	5.7	5.775	5.82

around. It is shown that even if the topology dynamically changes, accuracy converges to the same value. When comparing among topologies, the accuracy of R3 was slightly better than those of R2, BA2, and dynamic BA. Whereas the accuracies of R1 and BA1 were worse than that of others. These differences come from the algebraic connectivity λ_2 in (26) and (28). Table IV shows the algebraic connectivities and average degrees of the evaluated topologies. Since the connectivities of R2, BA2, and dynamic BA are close, they achieved similar performance. Similarly, the accuracies of R1 and BA1 are close because they have similar connectivities.

When evaluating ring topologies, adjacent devices have the same labels when evaluating ring networks, whereas randomly selected labels are distributed when evaluating BA networks. Despite such data-distribution difference, they achieve similar accuracies if the connectivities of the topologies are nearly the same. Therefore, it can be said that data distribution similarity among adjacent devices does not affect accuracy.

D. Scalability to the number of devices

Fig. 7 shows the average of accuracies and distillation losses with various numbers of devices. Distillation loss is MSE $c(\hat{w}_i)$ defined in (29). This metric indicates a similarity of NN models among adjacent devices. Topologies varied at each epoch by BA algorithm, but the number of all edges was kept stable. The connectivities with the different numbers of devices are listed in Table V. The listed algebraic connectivities are the averages of 100 randomly generated graphs. When evaluating MNIST, the learning and sharing rates were set to 0.01 and 0.1, respectively. Both rates were set to 0.1 when evaluating F-MNIST. Fig. 7 shows that even when the number of devices increased, NN models converged at nearly the same rate. This is because the averages of algebraic connectivity are approximately the same regardless of the number of devices as shown in Table V. These results infer that the proposed

algorithm works with a large number of devices as long as the connectivity does not drastically change.

V. CONCLUSION

We proposed a model-free federated learning scheme for IoE devices connected via multi-hop networks. We developed a meta-algorithm of a consensus-based optimization in a function space that optimizes the loss function in a distributed manner. The convergence of the meta-algorithm in a function space was mathematically analyzed using federated functions. Federated functions represented the joint status of the whole system, enabled us to obtain an upper bound of the distance among the local prediction functions. Then, we proposed a CMFD as an implementation of the meta-algorithm, which realized function aggregation among adjacent devices by leveraging a distillation method. We showed the CMFD achieved higher prediction accuracy and stability than a typical parameter-aggregation-based FL when the multi-hop network is weakly connected.

Our future work includes improving the algorithm by estimating the reliability of the local prediction functions. When training data is non-IID, there is a training bias among devices depending on data distributions. Although CMFD does not care about the reliability of the prediction accuracy of each label, the learning speed is expected to increase if weighted averaging is adopted when aggregating functions. In order to calculate the optimal weight, we will develop a method of estimating how well the local prediction function is trained.

APPENDIX A PROOF OF LEMMA 1

Let $a_i^m(x)$ and $a^m(x)$ represent the m th element of the real vector $a_i(x) \in \mathcal{Y}$ and a real vector defined as $(a_1^m(x), \dots, a_n^m(x))^T \in \mathbb{R}^n$, respectively. $\|Aa\|_{\Phi_n}^2$ can be derived as follows:

$$\begin{aligned} \|Aa\|_{\Phi_n}^2 &= \int_{\mathcal{X}} \sum_{m=1}^M \|Aa^m(x)\|_{\mathbb{R}^n}^2 d\mu \\ &\stackrel{(18)}{\leq} \int_{\mathcal{X}} \sum_{m=1}^M \|A\|^2 \|a^m(x)\|_{\mathbb{R}^n}^2 d\mu \\ &= \|A\|^2 \|a\|_{\Phi_n}^2. \end{aligned} \tag{31}$$

Taking square roots of both sides, we have $\|Aa\|_{\Phi_n} \leq \|A\| \|a\|_{\Phi_n}$.

Let v_i be the i th element of $\arg \max_{v \in \mathbb{R}^n} \left\{ \frac{\|Av\|}{\|v\|} \right\}$. If \hat{a} is defined as $\hat{a}_i^m(x) \equiv v_i$ for all m and x , \hat{a} satisfies $\|A\hat{a}\|_{\Phi_n} = \|A\| \| \hat{a} \|_{\Phi_n}$. Therefore, $\|A\|$ is the induced 2-norm corresponding to Φ_n .

APPENDIX B PROOF OF THEOREM 1

Substituting (20) into (21), the federated function f_{t+1} is derived as follows:

$$\begin{aligned} f_{t+1} &= P f_t - \eta_t P d_t \\ &= P^t f_1 - \sum_{\tau=1}^t \eta_\tau P^{t-\tau+1} d_\tau, \end{aligned} \tag{32}$$

where P is defined as $P := I - \varepsilon L$. Since $\mathbb{1}_{n \times n} L = \mathbf{0}$, we have $\mathbb{1}_{n \times n} P^t = \mathbb{1}_{n \times n} (\forall t \in \mathbb{N})$, where $\mathbf{0}$ represents the zero matrix. Therefore, the mean federated function \bar{f}_{t+1} is expressed as follows:

$$\bar{f}_{t+1} = \frac{1}{n} \mathbb{1}_{n \times n} \mathbf{f}_{t+1} = \bar{f}_1 - \sum_{\tau=1}^t \eta_\tau \bar{\mathbf{d}}_\tau. \quad (33)$$

Now, distance between \mathbf{f}_{t+1} and \bar{f}_{t+1} is bounded as follows:

$$\begin{aligned} & \|\mathbf{f}_{t+1} - \bar{f}_{t+1}\|_{\Phi_n} \\ &= \left\| P^t \mathbf{f}_1 - \sum_{\tau=1}^t \eta_\tau P^{t-\tau+1} \mathbf{d}_\tau - \bar{f}_1 + \sum_{\tau=1}^t \eta_\tau \bar{\mathbf{d}}_\tau \right\|_{\Phi_n} \\ &\leq \|Q_t \mathbf{f}_1\|_{\Phi_n} + \sum_{\tau=1}^t \eta_\tau \|Q_{t-\tau+1} \mathbf{d}_\tau\|_{\Phi_n}, \end{aligned} \quad (34)$$

where Q_t is defined as $Q_t := P^t - \frac{1}{n} \mathbb{1}_{n \times n}$. Using Lemma 1, (34) can be derived as follows:

$$\begin{aligned} & \|\mathbf{f}_{t+1} - \bar{f}_{t+1}\|_{\Phi_n} \\ &\leq \|Q_t\| \|\mathbf{f}_1\|_{\Phi_n} + \sum_{\tau=1}^t \eta_\tau \|Q_{t-\tau+1}\| \|\mathbf{d}_\tau\|_{\Phi_n}. \end{aligned} \quad (35)$$

Next, we consider the upper bound of Q_t . Using spectral decomposition, L can be written as $L = \sum_{i=1}^n \lambda_i u_i u_i^\top$, where λ_i and u_i the i th smallest eigenvalues and the corresponding orthonormal eigenvectors of L , respectively. Since the network graph is connected, the smallest eigenvalue and the corresponding eigenvector satisfies $\lambda_1 = 0, u_1 = \frac{1}{\sqrt{n}} \mathbb{1}_n$. Now, we can obtain the eigenvalues of Q_t as follows:

$$P = I - \varepsilon \sum_{i=1}^n \lambda_i u_i u_i^\top = \sum_{i=1}^n (1 - \varepsilon \lambda_i) u_i u_i^\top, \quad (36)$$

$$Q_t = \sum_{i=1}^n (1 - \varepsilon \lambda_i)^t u_i u_i^\top - \frac{1}{n} \mathbb{1}_{n \times n} = \sum_{i=2}^n \kappa_i^t u_i u_i^\top, \quad (37)$$

where κ_i denotes $1 - \varepsilon \lambda_i$. Thus, the eigenvalues of Q_t become 0 and κ_i^t for $i \geq 2$. Considering that L is symmetric, Q_t is also symmetric. Therefore, induced norm $\|Q_t\|$ is equal to the largest eigenvalues of Q_t in absolute. Since the network graph is connected, λ_i satisfies $0 < \lambda_i \leq 2\Delta$ for $i \geq 2$. Therefore, if ε satisfies $0 < \varepsilon \leq \frac{1}{2\Delta}$, we have $0 \leq \kappa_i < 1$. Now, we have $\|Q_t\| = \max\{0, \kappa_2^t, \dots, \kappa_n^t\} = \kappa_2^t$ because κ_i monotonically decreases.

Next, we derive an upper bound of $\|\mathbf{d}_t\|_{\Phi_n}$. Let $d \in \partial \mathcal{L}_{\mu_i}(f)$ denote a Fréchet subgradient of $\mathcal{L}_{\mu_i}(f)$. Using Lipschitz constant K_i of $\mathcal{L}_{\mu_i}(f)$ and the supremum S_i of ν_i , an upper bound of $\|d\nu_i\|_{L_\mu^2}$ is obtained as follows:

$$\|d\nu_i\|_{L_\mu^2} = \sqrt{\int_{\mathcal{X}} \|d\|_{\mathcal{Y}}^2 (\nu_i)^2 d\mu} \leq S_i K_i. \quad (38)$$

Now, an upper bound of $\|\mathbf{d}_t\|_{\Phi_n}$ can be obtained as follows:

$$\|\mathbf{d}_t\|_{\Phi_n} = \sqrt{\sum_{i=2}^n \|d_i^t \nu_i\|_{L_\mu^2}^2} \leq \sqrt{n} K_m, \quad (39)$$

where K_m is defined as $K_m := \max_i \{S_i K_i\}$. Now, an upper bound of $\|\mathbf{f}_{t+1} - \bar{f}_{t+1}\|_{\Phi_n}$ is obtained as follows:

$$\begin{aligned} & \|\mathbf{f}_{t+1} - \bar{f}_{t+1}\|_{\Phi_n} \\ &\leq \|\mathbf{f}_1\|_{\Phi_n} \kappa_2^t + \sqrt{n} K_m \sum_{\tau=1}^t \eta_\tau \kappa_2^{t-\tau+1}. \end{aligned} \quad (40)$$

Thus, we have the upper bound of the root-mean square distance D_t as follows:

$$\begin{aligned} D_t &= \frac{1}{\sqrt{n}} \|\mathbf{f}_t - \bar{f}_t\|_{\Phi_n} \\ &\leq \frac{1}{\sqrt{n}} \|\mathbf{f}_1\|_{\Phi_n} \kappa_2^{t-1} + K_m \sum_{\tau=1}^{t-1} \eta_\tau \kappa_2^{t-\tau}. \end{aligned} \quad (41)$$

APPENDIX C PROOF OF THEOREM 2

Since the average of f_i^t is written as $\bar{f}_{t+1} = \bar{f}_t - \eta_t \bar{\mathbf{d}}_t$, we have

$$\begin{aligned} & \|\bar{f}_{t+1} - f^*\|_{L_\mu^2}^2 \\ &= \|\bar{f}_t - f^*\|_{L_\mu^2}^2 - 2\eta_t \langle \bar{\mathbf{d}}_t, \bar{f}_t - f^* \rangle_{L_\mu^2} + \eta_t^2 \|\bar{\mathbf{d}}_t\|_{L_\mu^2}^2. \end{aligned} \quad (42)$$

The second term of the right hand side of (42) is derived as follows:

$$\begin{aligned} & - \langle \bar{\mathbf{d}}_t, \bar{f}_t - f^* \rangle_{L_\mu^2} \\ &= \frac{1}{n} \sum_i \langle d_i^t \nu_i, f^* - \bar{f}_t \rangle_{L_\mu^2} \\ &= \frac{1}{n} \sum_i \left[\langle d_i^t \nu_i, f^* - f_i^t \rangle_{L_\mu^2} + \langle d_i^t \nu_i, f_i^t - \bar{f}_t \rangle_{L_\mu^2} \right]. \end{aligned} \quad (43)$$

Using Cauchy–Schwarz inequality, we have

$$\begin{aligned} \langle d_i^t \nu_i, f_i^t - \bar{f}_t \rangle_{L_\mu^2} &\leq \|d_i^t \nu_i\|_{L_\mu^2} \|f_i^t - \bar{f}_t\|_{L_\mu^2} \\ &\stackrel{(38)}{\leq} K_m \|f_i^t - \bar{f}_t\|_{L_\mu^2}. \end{aligned} \quad (44)$$

Using Radon-Nikodym derivative $\nu_i = \frac{d\mu_i}{d\mu}$, (16) can be rewritten as follows:

$$\forall h \in L_{\mu_i}^2, \langle d_i^t \nu_i, h - f_i^t \rangle_{L_\mu^2} \leq \mathcal{L}_{\mu_i}(h) - \mathcal{L}_{\mu_i}(f_i^t). \quad (45)$$

Choosing f^* as h , we have

$$\begin{aligned} & \langle d_i^t \nu_i, f^* - f_i^t \rangle_{L_\mu^2} \\ &\leq \mathcal{L}_{\mu_i}(f^*) - \mathcal{L}_{\mu_i}(f_i^t) \\ &\leq \mathcal{L}_{\mu_i}(f^*) - \mathcal{L}_{\mu_i}(\bar{f}_t) + \mathcal{L}_{\mu_i}(\bar{f}_t) - \mathcal{L}_{\mu_i}(f_i^t). \end{aligned} \quad (46)$$

Here, let $d_{\bar{f}_t}$ denote a Fréchet subgradient of $\mathcal{L}_{\mu_i}(\bar{f}_t)$, then the $d_{\bar{f}_t}$ satisfies the following inequality:

$$\forall h, \langle d_{\bar{f}_t}, h - \bar{f}_t \rangle_{L_\mu^2} \leq \mathcal{L}_{\mu_i}(h) - \mathcal{L}_{\mu_i}(\bar{f}_t). \quad (47)$$

If we choose f_i^t as h , we have

$$\begin{aligned}
 \mathbb{L}_{\mu_i}(\bar{f}_t) - \mathbb{L}_{\mu_i}(f_i^t) &\leq \langle d_{\bar{f}_t}, \bar{f}_t - f_i^t \rangle_{L_{\mu_i}^2} \\
 &= \langle d_{\bar{f}_t} \nu_i, \bar{f}_t - f_i^t \rangle_{L_{\mu_i}^2} \\
 &\leq \|d_{\bar{f}_t} \nu_i\|_{L_{\mu_i}^2} \|\bar{f}_t - f_i^t\|_{L_{\mu_i}^2} \\
 &\stackrel{(38)}{\leq} K_m \|f_i^t - \bar{f}_t\|_{L_{\mu_i}^2} \\
 &\leq \sqrt{n} K_m \gamma_t. \tag{48}
 \end{aligned}$$

In the above inequality, we used $\|f_i^t - \bar{f}_t\|_{L_{\mu_i}^2} \leq \|f_t - \bar{f}_t\|_{\Phi_n}$. Substituting (44), (46), and (48) into (43), and using (8), we obtain the following inequality:

$$\begin{aligned}
 & - \langle \bar{d}_t, \bar{f}_t - f^* \rangle_{L_{\mu}^2} \\
 & \leq \frac{1}{n} \sum_i^n [\mathbb{L}_{\mu_i}(f^*) - \mathbb{L}_{\mu_i}(\bar{f}_t) + 2\sqrt{n} K_m \gamma_t] \\
 & \leq \mathbb{L}_{\mu}(f^*) - \mathbb{L}_{\mu}(\bar{f}_t) + 2\sqrt{n} K_m \gamma_t. \tag{49}
 \end{aligned}$$

Now, (42) can be derived as follow:

$$\begin{aligned}
 & \|\bar{f}_{t+1} - f^*\|_{L_{\mu}^2}^2 \\
 & \leq \|\bar{f}_t - f^*\|_{L_{\mu}^2}^2 + \eta_t^2 K_m \\
 & \quad + 2\eta_t [\mathbb{L}_{\mu}(f^*) - \mathbb{L}_{\mu}(\bar{f}_t) + 2\sqrt{n} K_m \gamma_t] \\
 & \leq \|\bar{f}_2 - f^*\|_{L_{\mu}^2}^2 + K_m \sum_{\tau=2}^t \eta_{\tau}^2 + 4\sqrt{n} K_m \sum_{\tau=2}^t \eta_{\tau} \gamma_{\tau} \\
 & \quad + 2 \sum_{\tau=2}^t \eta_{\tau} [\mathbb{L}_{\mu}(f^*) - \mathbb{L}_{\mu}(\bar{f}_{\tau})]. \tag{50}
 \end{aligned}$$

Using $\|\bar{f}_{t+1} - f^*\|_{L_{\mu}^2}^2 \leq 0$ and $C_1 := \|\bar{f}_2 - f^*\|_{L_{\mu}^2}^2$, we have

$$\begin{aligned}
 \mathbb{L}_{\mu}(f_{\text{best},t}) - \mathbb{L}_{\mu}(f^*) &= \min_{\tau=1, \dots, t} \{\mathbb{L}_{\mu}(\bar{f}_{\tau})\} - \mathbb{L}_{\mu}(f^*) \\
 &\leq \frac{C_1 + K_m \sum_{\tau=2}^t \eta_{\tau}^2 + 4\sqrt{n} K_m \sum_{\tau=2}^t \eta_{\tau} \gamma_{\tau}}{2 \sum_{\tau=2}^t \eta_{\tau}}. \tag{51}
 \end{aligned}$$

An upper bound of $\sum_{\tau=2}^t \eta_{\tau} \gamma_{\tau}$ is obtained as follows:

$$\begin{aligned}
 \sum_{\tau=2}^t \eta_{\tau} \gamma_{\tau} &= \frac{1}{\sqrt{n}} \|\mathbf{f}_1\|_{\Phi_n} \sum_{\tau=2}^t \eta_{\tau} \kappa_2^{\tau-1} \\
 &\quad + K_m \sum_{\tau=2}^t \sum_{\tau'=1}^{\tau-1} \eta_{\tau} \eta_{\tau'} \kappa_2^{\tau-\tau'}. \tag{52}
 \end{aligned}$$

Using the monotonicity of η_t , the second term of the right hand side is upper bounded as follows:

$$\begin{aligned}
 \sum_{\tau=2}^t \sum_{\tau'=1}^{\tau-1} \eta_{\tau} \eta_{\tau'} \kappa_2^{\tau-\tau'} &= \sum_{\tau'=1}^{t-1} \sum_{\tau=1}^{t-\tau'} \eta_{\tau+\tau'} \eta_{\tau} \kappa_2^{\tau'} \\
 &\leq \sum_{\tau'=1}^{t-1} \sum_{\tau=1}^{t-1} \eta_{\tau}^2 \kappa_2^{\tau'} \\
 &= \frac{\kappa_2(1 - \kappa_2^{t-1})}{1 - \kappa_2} \sum_{\tau=1}^{t-1} \eta_{\tau}^2. \tag{53}
 \end{aligned}$$

Thus, we have

$$\sum_{\tau=2}^t \eta_{\tau} \gamma_{\tau} \leq \frac{\kappa_2(1 - \kappa_2^{t-1})}{1 - \kappa_2} \left(\frac{\eta_1}{\sqrt{n}} \|\mathbf{f}_1\|_{\Phi_n} + K_m \sum_{\tau=1}^{t-1} \eta_{\tau}^2 \right). \tag{54}$$

Now, (51) can be derived as follows:

$$\begin{aligned}
 & \mathbb{L}_{\mu}(f_{\text{best},t}) - \mathbb{L}_{\mu}(f^*) \\
 & \leq \frac{1}{2 \sum_{\tau=2}^t \eta_{\tau}} \left[C_1 + K_m \sum_{\tau=2}^t \eta_{\tau}^2 \right. \\
 & \quad \left. + C_2 (1 - \kappa_2^{t-1}) \left(\eta_1 \|\mathbf{f}_1\|_{\Phi_n} + \sqrt{n} K_m \sum_{\tau=1}^{t-1} \eta_{\tau}^2 \right) \right], \tag{55}
 \end{aligned}$$

where C_2 is defined as $C_2 := \frac{4K_m \kappa_2}{1 - \kappa_2}$.

REFERENCES

- [1] B. McMahan, E. Moore, D. Ramage, S. Hampson, and B. A. y Arcas, "Communication-efficient learning of deep networks from decentralized data," in *Proc. of the 20th International Conference on Artificial Intelligence and Statistics (AISTATS)*, Fort Lauderdale, FL, USA, Apr. 2017, pp. 1273–1282.
- [2] P. Kairouz, H. B. McMahan, B. Avent, A. Bellet, M. Bennis, A. N. Bhagoji, K. Bonawitz, Z. Charles, G. Cormode, R. Cummings *et al.*, "Advances and open problems in federated learning," *arXiv preprint arXiv:1912.04977*, Dec. 2019.
- [3] S. Savazzi, M. Nicoli, and V. Rampa, "Federated learning with cooperating devices: A consensus approach for massive IoT networks," *IEEE Internet of Things Journal*, vol. 7, no. 5, pp. 4641–4654, May 2020.
- [4] A. Lalitha, O. C. Kilinc, T. Javidi, and F. Koushanfar, "Peer-to-peer federated learning on graphs," *arXiv preprint arXiv:1901.11173*, Jan. 2019.
- [5] X. Lian, C. Zhang, H. Zhang, C.-J. Hsieh, W. Zhang, and J. Liu, "Can decentralized algorithms outperform centralized algorithms? a case study for decentralized parallel stochastic gradient descent," in *Proc. of the 31st Conference on Neural Information Processing Systems (NeurIPS 2017)*, Long Beach, CA, USA, Dec. 2017, pp. 5330–5340.
- [6] K. Sato, Y. Satoh, and D. Sugimura, "Network-density-controlled decentralized parallel stochastic gradient descent in wireless systems," in *Proc. of 2020 IEEE International Conference on Communications (ICC)*, Virtual Conference, Jun. 2020.
- [7] S. Oh, J. Park, E. Jeong, H. Kim, M. Bennis, and S.-L. Kim, "Mix2FLD: downlink federated learning after uplink federated distillation with two-way mixup," *IEEE Communications Letters*, vol. 24, no. 10, pp. 2211–2215, Jun. 2020.
- [8] J.-H. Ahn, O. Simeone, and J. Kang, "Wireless federated distillation for distributed edge learning with heterogeneous data," in *Proc. of 2019 IEEE 30th Annual International Symposium on Personal, Indoor and Mobile Radio Communications (PIMRC)*, Istanbul, Turkey, Nov. 2019, pp. 1–6.
- [9] S. Itahara, T. Nishio, Y. Koda, M. Morikura, and K. Yamamoto, "Distillation-based semi-supervised federated learning for communication-efficient collaborative training with non-IID private data," *arXiv preprint arXiv:2008.06180*, Aug. 2020.
- [10] E. Jeong, S. Oh, H. Kim, J. Park, M. Bennis, and S.-L. Kim, "Communication-efficient on-device machine learning: Federated distillation and augmentation under non-IID private data," *arXiv preprint arXiv:1811.11479*, Nov. 2018.
- [11] H. Chang, V. Shejwalkar, R. Shokri, and A. Houmansadr, "Cronus: Robust and heterogeneous collaborative learning with black-box knowledge transfer," *arXiv preprint arXiv:1912.11279*, Dec. 2019.
- [12] E. Jeong, S. Oh, J. Park, H. Kim, M. Bennis, and S.-L. Kim, "Multi-hop federated private data augmentation with sample compression," *arXiv preprint arXiv:1907.06426*, Jul. 2019.
- [13] R. Anil, G. Pereyra, A. Passos, R. Ormandi, G. E. Dahl, and G. E. Hinton, "Large scale distributed neural network training through online distillation," *arXiv preprint arXiv:1804.03235*, Apr. 2018.
- [14] Y. Zhang, T. Xiang, T. M. Hospedales, and H. Lu, "Deep mutual learning," in *Proc. of 2018 IEEE/CVF Conference on Computer Vision and Pattern Recognition (CVPR)*. IEEE, 2018, pp. 4320–4328.

- [15] Y. Zhao, M. Li, L. Lai, N. Suda, D. Civin, and V. Chandra, "Federated learning with non-IID data," *arXiv preprint arXiv:1806.00582*, Jun. 2018.
- [16] F. Sattler, S. Wiedemann, K.-R. Müller, and W. Samek, "Robust and communication-efficient federated learning from non-i.i.d. data," *IEEE Transactions on Neural Networks and Learning Systems*, vol. 31, no. 9, pp. 3400–3413, Sep. 2020.
- [17] X. Li, K. Huang, W. Yang, S. Wang, and Z. Zhang, "On the convergence of FedAvg on non-IID data," in *Proc. of the 7th International Conference on Learning Representations (ICLR)*, Online Conference, Apr. 2020.
- [18] C. Buciluă, R. Caruana, and A. Niculescu-Mizil, "Model compression," in *Proc. of the 12th ACM SIGKDD international conference on Knowledge discovery and data mining*, Philadelphia, USA, Aug. 2006, pp. 535–541.
- [19] J. Park, S. Samarakoon, M. Bennis, , and M. Debbah, "Wireless network intelligence at the edge," *Proceedings of the IEEE*, vol. 107, no. 11, pp. 2204–2239, Nov. 2019.
- [20] J. Park, S. Wang, A. Elgabli, S. Oh, E. Jeong, H. Cha, H. Kim, S.-L. Kim, and M. Bennis, "Distilling on-device intelligence at the network edge," *arXiv preprint arXiv:1908.05895*, Aug. 2019.
- [21] A. Nedic and A. Ozdaglar, "Distributed subgradient methods for multi-agent optimization," *IEEE Transactions on Automatic Control*, vol. 54, no. 1, pp. 48–61, Jan. 2009.
- [22] B. Johansson, M. Rabi, and M. Johansson, "A randomized incremental subgradient method for distributed optimization in networked systems," *SIAM Journal on Optimization*, vol. 20, no. 3, pp. 1157–1170, Aug. 2009.
- [23] I. Colin, A. Bellet, J. Salmon, and S. Cléménçon, "Gossip dual averaging for decentralized optimization of pairwise functions," in *Proc. of the 33rd International Conference on Machine Learning (ICML)*, New York, USA, Jun. 2016, pp. 1388–1396.
- [24] A. Elgabli, J. Park, A. S. Bedi, M. Bennis, and V. Aggarwal, "GADMM: Fast and communication efficient framework for distributed machine learning," *Journal of Machine Learning Research*, vol. 21, no. 76, pp. 1–39, Mar. 2020.
- [25] T. Van Erven and P. Harremos, "Rényi divergence and Kullback-Leibler divergence," *IEEE Transactions on Information Theory*, vol. 60, no. 7, pp. 3797–3820, Jul. 2014.
- [26] L. Ambrosio, N. Gigli, and G. Savaré, *Gradient flows: in metric spaces and in the space of probability measures*. Springer Science & Business Media, 2008.
- [27] M. Fiedler, "Algebraic connectivity of graphs," *Czechoslovak mathematical journal*, vol. 23, no. 2, pp. 298–305, 1973.
- [28] S. Boyd, L. Xiao, and A. Mutapcic, "Subgradient methods," *lecture notes of EE392o, Stanford University, Autumn Quarter*, 2003–2004.
- [29] Y. LeCun, L. Bottou, Y. Bengio, and P. Haffner, "Gradient-based learning applied to document recognition," *Proceedings of the IEEE*, vol. 86, no. 11, pp. 2278–2324, Nov. 1998.
- [30] H. Xiao, K. Rasul, and R. Vollgraf, "Fashion-MNIST: a novel image dataset for benchmarking machine learning algorithms," *arXiv preprint arXiv:1708.07747*, 2017.
- [31] H. Zhu, H. Luo, H. Peng, L. Li, and Q. Luo, "Complex networks-based energy-efficient evolution model for wireless sensor networks," *Chaos, Solitons & Fractals*, vol. 41, no. 4, pp. 1828–1835, Aug. 2009.
- [32] A.-L. Barabási and R. Albert, "Emergence of scaling in random networks," *Science*, vol. 286, no. 5439, pp. 509–512, Oct. 1999.



Akihito Taya (S'12–M'17) received the B.E. degree in electrical and electronic engineering from Kyoto University, Kyoto, Japan in 2011, and the master and Ph.D. degree in Informatics from Kyoto University in 2013 and 2019, respectively. From 2013 to 2017, He joined Hitachi, Ltd., where he participated in the development of computer clusters. He has been an assistant professor of the Aoyama Gakuin University, since 2019. He received the IEEE VTS Japan Young Researcher's Encouragement Award and the IEICE Young Researcher's Award in 2012

and 2018, respectively. His current research interests include distributed machine learning and human activity and emotion recognition using sensor networks. He is a member of the IEEE, ACM, and IEICE.



Takayuki Nishio (S'11–M'14–SM'20) has been an associate professor in the School of Engineering, Tokyo Institute of Technology, Japan, since 2020. He received the B.E. degree in electrical and electronic engineering and the master's and Ph.D. degrees in informatics from Kyoto University in 2010, 2012, and 2013, respectively. He had been an assistant professor in the Graduate School of Informatics, Kyoto University from 2013 to 2020. From 2016 to 2017, he was a visiting researcher in Wireless Information Network Laboratory (WINLAB), Rutgers University, United States. His current research interests include machine learning-based network control, machine learning in wireless networks, and heterogeneous resource management.



Masahiro Morikura (M'82) received B.E., M.E. and Ph.D. degree in electronic engineering from Kyoto University, Kyoto, Japan in 1979, 1981 and 1991, respectively. He joined NTT in 1981, where he was engaged in the research and development of TDMA equipment for satellite communications. From 1988 to 1989, he was with the communications Research Centre, Canada as a guest scientist. From 1997 to 2002, he was active in standardization of the IEEE802.11a based wireless LAN. He received Paper Award, Achievement Award and Distinguished

Achievement and Contributions Award from the IEICE in 2000, 2006 and 2019, respectively. He also received Education, Culture, Sports, Science and Technology Minister Award in 2007 and Maejima Award from the Teishin association in 2008 and the Medal of Honor with Purple Ribbon from Japan's Cabinet Office in 2015. Dr. Morikura is now a professor of the Graduate School of Informatics, Kyoto University. He is a Fellow of the IEICE and a member of IEEE.



Koji Yamamoto (S'03–M'06–SM'20) received the B.E. degree in electrical and electronic engineering from Kyoto University in 2002, and the master and Ph.D. degrees in Informatics from Kyoto University in 2004 and 2005, respectively. From 2004 to 2005, he was a research fellow of the Japan Society for the Promotion of Science (JSPS). Since 2005, he has been with the Graduate School of Informatics, Kyoto University, where he is currently an associate professor. From 2008 to 2009, he was a visiting researcher at Wireless@KTH, Royal Institute of

Technology (KTH) in Sweden. He serves as an editor of IEEE Wireless Communications Letters, IEEE Open Journal of Vehicular Technology, and Journal of Communications and Information Networks, a symposium co-chair of GLOBECOM 2021, and a vice co-chair of IEEE ComSoc APB CCC. He was a tutorial lecturer in ICC 2019. His research interests include radio resource management, game theory, and machine learning. He received the PIMRC 2004 Best Student Paper Award in 2004, the Ericsson Young Scientist Award in 2006. He also received the Young Researcher's Award, the Paper Award, SUEMATSU-Yasuharu Award, Educational Service Award from the IEICE of Japan in 2008, 2011, 2016, and 2020, respectively, and IEEE Kansai Section GOLD Award in 2012. He is a senior member of the IEICE and a member of the Operations Research Society of Japan.